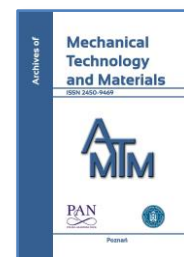


DE GRUYTER  
OPEN

ARCHIVES OF MECHANICAL TECHNOLOGY AND MATERIALS

WWW.AMTM.PUT.POZNAN.PL



## Open loop control of piezoelectric tube transducer

Frederik Stefanski<sup>a\*</sup>, Bartosz Minorowicz<sup>a</sup><sup>a</sup>Faculty of Mechanical Engineering and Management, Institute of Mechanical Technology, Poznan University of Technology, Piotrowo Street 3, Poznan 60-965, Poland

\*Corresponding author, e-mail address: frederik.stefanski@gmail.com

### ARTICLE INFO

Received 31 May 2017  
Received in revised form 10 April 2018  
Accepted 29 May 2018

### KEY WORDS

Piezoelectric actuator  
Open loop control  
Hysteresis  
Generalized Prandtl-Ishlinski model  
Hysteresis compensation

### ABSTRACT

This paper is focused on the open loop control of a piezoelectric tube actuator, hindered by a strong hysteresis. The actuator was distinguished with 22 % hysteresis, which hinders the positioning of piezoelectric actuator. One of the possible ways to solve this problem is application of an accurate analytical inversed model of the hysteresis in the control loop. In this paper generalized Prandtl-Ishlinskii model was used for both modeling and open loop control of the piezoelectric actuator. Achieved modeling error does not exceed max. 2.34 % of the whole range of tube deflection. Finally, the inverse hysteresis model was applied to the control line of the tube. For the same input signal (damped sine 0.2 Hz) as for the model estimation the positioning error was max. 4.6 % of the tube deflection. Additionally, for a verification reason three different complex harmonic functions were applied. For the verification functions, still a good positioning was obtained with positioning error of max. 4.56 %, 6.75 % and 5.6% of the tube deflection.

### 1. INTRODUCTION

Piezoelectric materials have had a wide range of applications, e.g. in micro- and nano-positioning stages [1,2], vibration control [3], fluid power pilot valves [4-6], energy harvesting [7,8], and other areas in which conventional solutions cannot fulfil the increasing requirements with regard to fast response, high precision, high speed positioning and low energy costs. Piezoelectric actuators use inversed piezoelectric effect which converses applied electrical field to the surface of the material into deformation of the material. Nowadays, piezoelectric materials are artificially synthesized for achieving high levels of piezoelectric effect. One of these materials is based on lead zirconate titanate (Pb(Zr,Ti)O<sub>3</sub> or PZT). This material exhibits superior piezo properties and can be divided into two main types depending on the applied element oxides, hard PZT and soft PZT. The first is distinguished by low hysteresis and energy losses, but can produce small displacements. In comparison, soft PZT, typically used for

actuators, can produce higher displacement but is hindered by considerable hysteresis and energy dissipation [9-11].

The hysteresis behavior of the material occurs between the applied electrical field and charge, and in effect between the applied voltage and PZT displacement. The hysteresis positioning error is typically about 10-25% of the full measurement range, and has been reported to increase up to 35% when the rate of the input signal increases [12,13]. Additionally, it is rate dependent, which means that the loop's shape will broaden when the input signal rate increases [14,15]. The hysteresis behavior causes significant positioning inaccuracy of the system in open-loop control. Furthermore, it degrades the tracing performance in closed-loop control systems. The hysteresis behavior is a dominant issue that has to be solved when application of piezo materials is considered [2,16].

### 2. PIEZOELECTRIC TUBE ACTUATOR

The PZT tube, which is used in this research, has a unique feature compared to other piezo actuators. This tube can

deform in three axes. Such complex movement is possible because this actuator can deflect along the X and Y axes and elongates along the Z axis depending on which electrodes are currently powered. Tubes can be used to develop advanced mechatronic devices and they are the foremost actuators used in scanning probe microscopes and atomic force microscopes.

### 2.1. ACTUATOR AND TEST BENCH

The test bench and the actuator are shown in scheme and photograph in Fig. 1. The aforementioned piezo actuator (1) is fixed in a nonconductive stiff mounting and mounted to the solid metal base (3). Precise displacement measurements are executed via a laser displacement sensor optoNCDT 1700 with 0.5  $\mu\text{m}$  resolution and a 2 mm measurement range (2). The number (4) is a two-channel high voltage amplifier with a two-channel control signal input (5). The high voltage amplifier was specially designed for these tests and is based on an APEX P91 high voltage operational amplifier. It has an amplification ratio of  $k_{amp} = 20$  with maximal output voltage  $U_z = \pm 200$  V per channel. Control, signal processing and data acquisition are performed using a dSPACE microcontroller board, 12 bit DAC output for the control signal and with 16-bit ADC input for the laser sensor. The system sampling frequency is 1000 Hz. The system is controlled in real time via a Matlab Simulink model implemented in PC connected to the dSPACE system. To reduce the influence of the environment, the whole test stand is placed on a vibration absorbing table. Supply voltage was applied to the piezoelectric tube on two opposite electrodes, as in Fig. 1, which will allow to deflect the free end of the tube in x axis. The remaining electrodes were connected to a common ground. The parameters of the actuator are presented in Table 1.

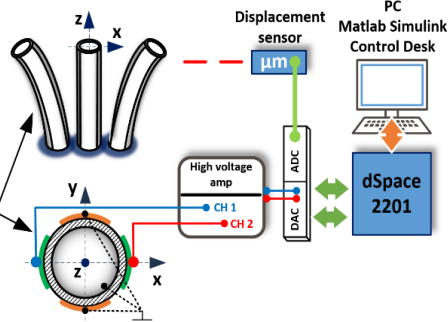
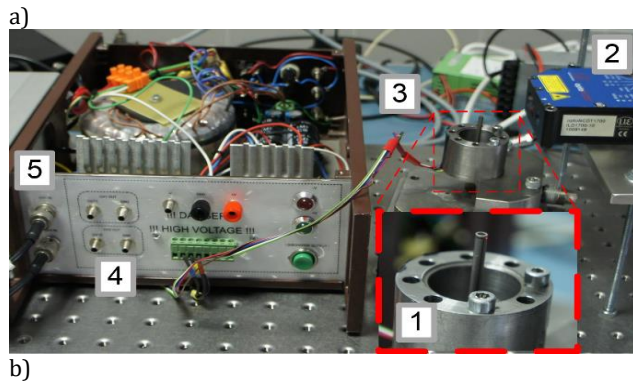


Fig. 1. Test stand a) photograph, b) scheme.

### 2.2. GENERALIZED PRANDTL-ISHLINSKI HYSTERESIS MODEL

In this paper, a generalized version of the Prandtl-Ishlinskii model (GPIM) is used. The GPI model was a topic of various papers, e.g. [17][18][19], and because of it, only a short introduction in this model is presented below. A discrete form of this model is presented in equation (1). The GPI model  $Y_{py}$  consists of a number of  $N$  play operators  $G_r(2)$  multiplied by density function  $p(r)$  described by equation (3). The play operator connects the input signal  $v$  with an output  $z$  and the relation between them is described by two envelop functions  $\gamma_r, \gamma_l$  and threshold  $r$ . The following operators and density functions are changing and dependent on value of  $j$ -threshold  $r$  described by (4).

Table 1. Actuator and system parameters

Description	Parameter	Unit	Value
Tube thickness	$h_p$	[m]	$0,5 \cdot 10^{-3}$
Tube outer diameter	$D_p$	[m]	$3,2 \cdot 10^{-3}$
Tube length	$L_p$	[m]	$35 \cdot 10^{-3}$
Piezoelectric coefficient	$d_{31}$	[m/V]	$-210 \cdot 10^{-12}$
Piezo constant	$K_v$	[m/V]	$-1.45 \cdot 10^{-7}$
Amplifier gain	$k_{amp}$	[-]	20
Control signal	$U_r$	[V]	-10 to 10
Supply voltage	$U_z$	[V]	-200 to 200

$$Y_{py}(t) = \sum_{j=0}^N p(r_j) \cdot G_{r_j}(v(t)) \quad (1)$$

$$G_r(v(t)) = \begin{cases} \max(\gamma_l(t) - r, z(v(t_i))), & \text{for } v(t) > v(t_i) \\ \min(\gamma_r(t) + r, z(v(t_i))), & \text{for } v(t) < v(t_i) \\ z(v(t_i)), & \text{for } v(t) = v(t_i) \end{cases} \quad (2)$$

$$p(r_j) = \rho e^{-\tau r_j} \quad (3)$$

$$r_j = \alpha j \quad (4)$$

where:  $\alpha, \rho, \tau$  are constant parameters of the model and  $j \in \langle 0; N \rangle$ .

If the shapes of the increasing and decreasing hysteresis slopes are very similar, simplifying the model by using the same envelop function to describe the increasing and decreasing shapes of the hysteresis can be considered as in (5). The advantages of this approach are faster parameter estimation, a simpler model.

$$\gamma_l(v) = \gamma_r(v) = a_0 v + a_1 \quad (5)$$

### 2.3. MODELING RESULTS

The  $\alpha, \rho, \tau, a_0, a_1$  parameters of the GPIM model were estimated on the base of measurement data acquired for a training input signal as in (6). This damped sine signal was used to get main and minor hysteresis loops and the relation between them. The parameters were estimated using a nonlinear least square estimation method available in Matlab Simulink software and are presented in Table 2.

$$U_r(t) = \begin{cases} 0 & dla \quad t \in (0; 4s) \wedge (69; 70s) \\ \sin(2\pi 0.2(t-4)) & dla \quad t \in (4; 19s) \\ \sin(2\pi 0.2(t-19)) \cdot (1-0.2(t-19)) & dla \quad t \in (19; 69s) \end{cases} \quad (6)$$

Table 2. GPI model parameters

Parameter	Value	Parameter	Value
$\alpha$	0.0066	$a0$	0.0066
$\rho$	36.6742	$a1$	-0.0592
$\tau$	-26.9790	$N$	15

The GPI model accuracy was presented in Fig. 2 in time and for control signal. Modelling error was calculated as the difference between the measurement and the GPIM output and showed in Fig. 2 c) and Table 3.

Table 3. Model error results

	Training signal	
	[ $\mu\text{m}$ ]	[%]
PZT tube strain range	118.5	100
Max. positive error	2.35	1.99
Max. negative error	-2.78	2.34

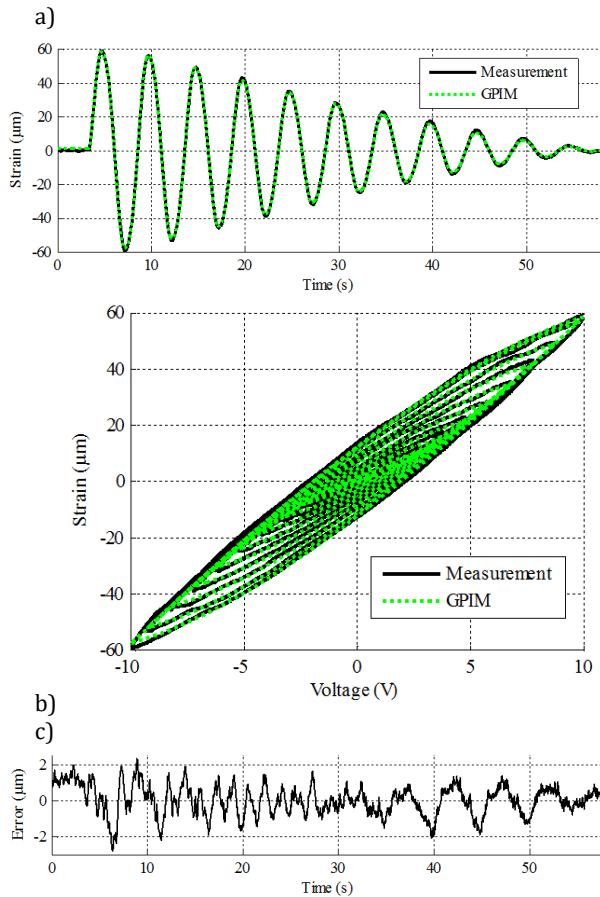


Fig. 2. Piezoelectric tube displacement and model a) in time, b) for the input voltage, c) modeling error in time.

### 3. PIEZOELECTRIC ACTUATOR OPEN LOOP CONTROL

The result in Fig. 2 shows a wide hysteresis (max. 22 % of the displacement range), which limits the precision of the piezo actuator positioning. To increase the positioning and

reduce the influence of the hysteresis an inverse Prandtl-Ishlinskii model (IGPIM) was used. The inverse hysteresis model  $H^{-1}$  will be applied to the open loop control system like in Fig. 3

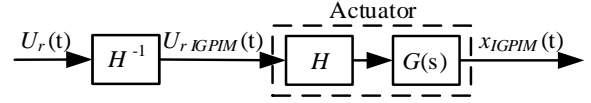


Fig. 3. Open loop control strategy

### 3.1. INVERSE GENERALIZED PRANDTL-ISHLINSKIIMODEL

Continuous and monolithic character of GPIM allows to achieve an exact analytical inverse version of this model. The inverse model can be described by equation (6). A wider mathematical description of this inversion can be found in [18,19].

$$Y_{pr}^{-1}(v) = \begin{cases} \gamma_l^{-1} \left( \sum_{i=0}^N \hat{p}_i F_{r_j}^+[v](t) \right) & dla \quad v(t) \geq 0 \\ \gamma_r^{-1} \left( \sum_{i=0}^N \hat{p}_i F_{r_j}^-[v](t) \right) & dla \quad v(t) \leq 0 \end{cases} \quad (6)$$

In the IGPIM an inverse density function is used described by equation (7) and an inverse threshold like in (8).

$$\hat{p}_j = - \frac{P_j}{\left( \sum_{i=0}^j P_i \right) \left( \sum_{i=0}^{j-1} P_i \right)} \quad (7)$$

for  $j = 1, 2, \dots, N$

$$\hat{r}_j = \sum_{i=0}^j p_i (r_j - r_i) \quad (8)$$

for  $j = 0, 1, \dots, N$

### 3.2. OPEN LOOP CONTROL RESULTS

The first open loop control test was performed for the same signal as for the model parameters estimation (eq. 6). The results were presented in figure 3a and 3b. Figure 3d shows the inverse model output for the control signal. The positioning error was calculated as the difference between the reference signal and the measured piezo tube displacement (Fig. 3c).

The second test was undertaken for verification for three different control signals with a more complex structure as the estimation signal. The signals F1, F2 and F3 were applied to the system and piezoelectric tube displacement was measured. The results are shown in Fig. 4 for signal F1, Fig. 5 for signal F2 and Fig. 6 for signal F3.

## 4. DISCUSSION AND CONCLUSIONS

The deflection of the free end of the tested actuator (Fig. 2) shows a strong hysteresis behavior which hinders the positioning in max. of 22 % of the range.

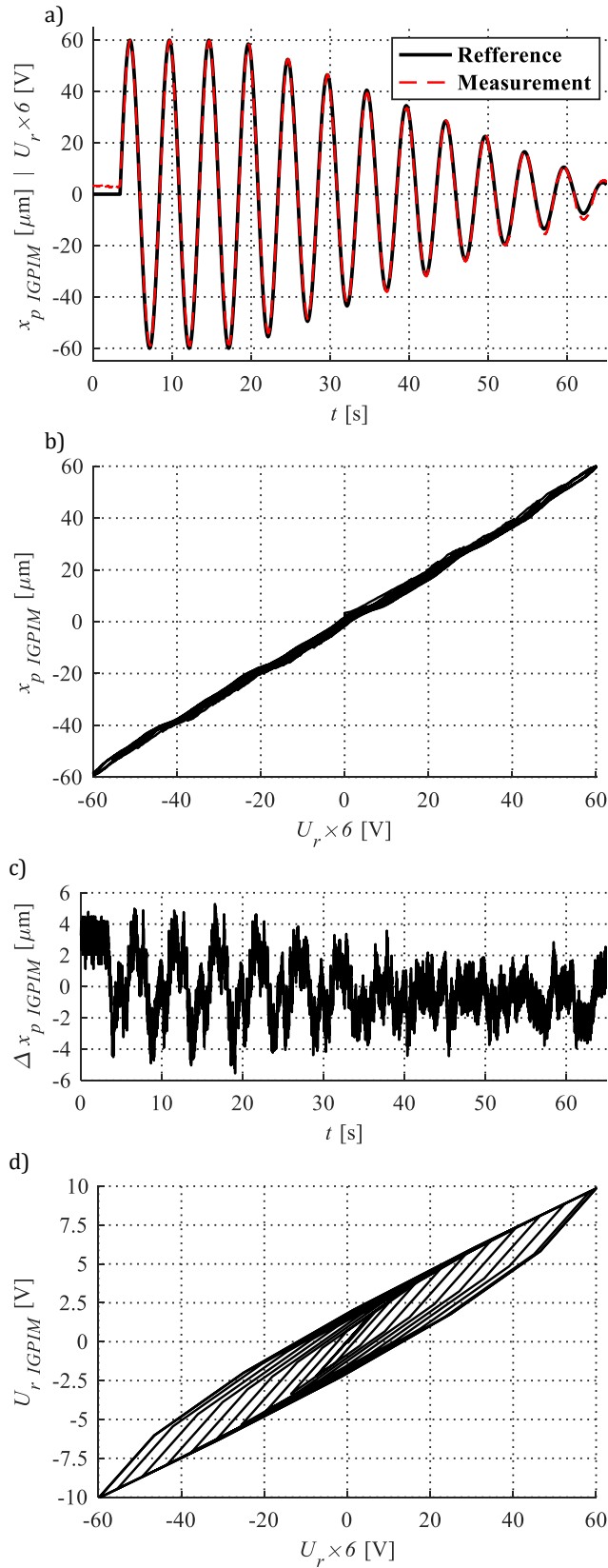


**Fig. 3.** Piezoelectric tube displacement for training signal a) in time, b) for control voltage, c) modeling error in time, d) IGPIM model output.

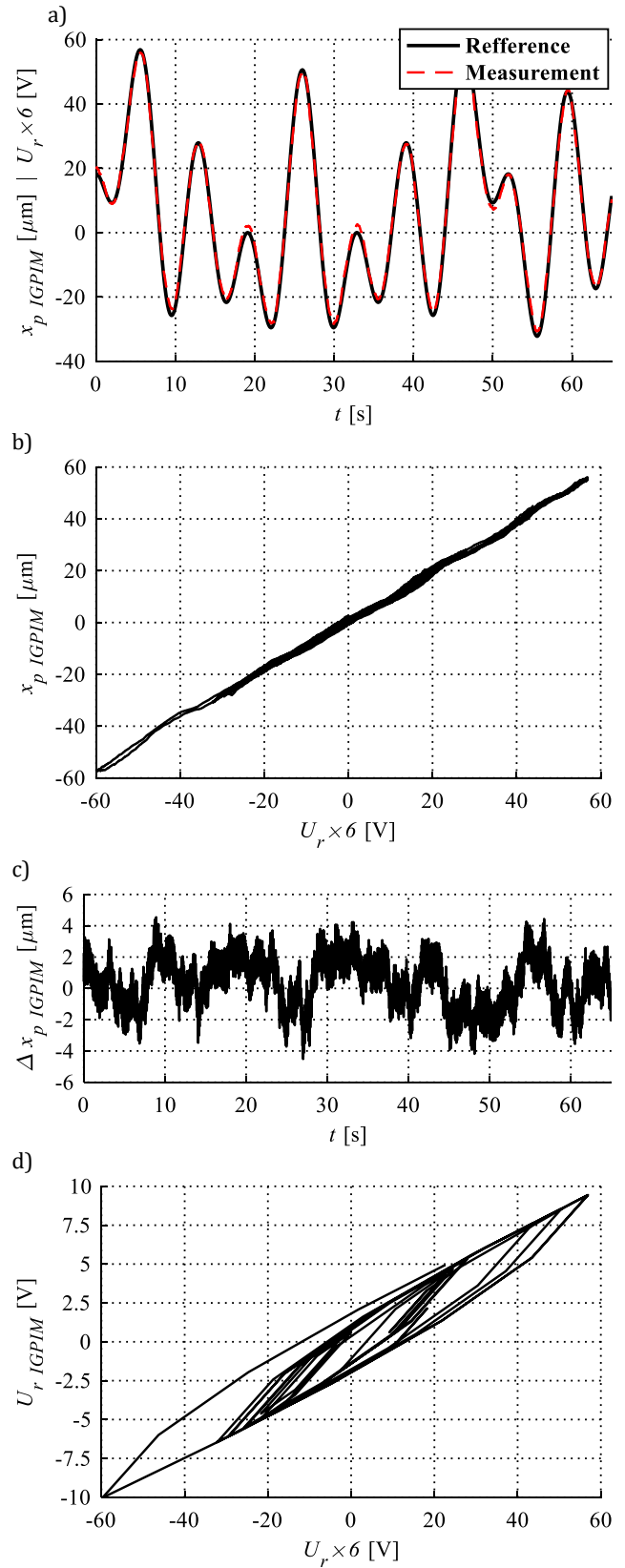


**Fig. 4.** Piezoelectric tube displacement for function F1 a) in time, b) for control voltage, c) modeling error in time, d) IGPIM model output.

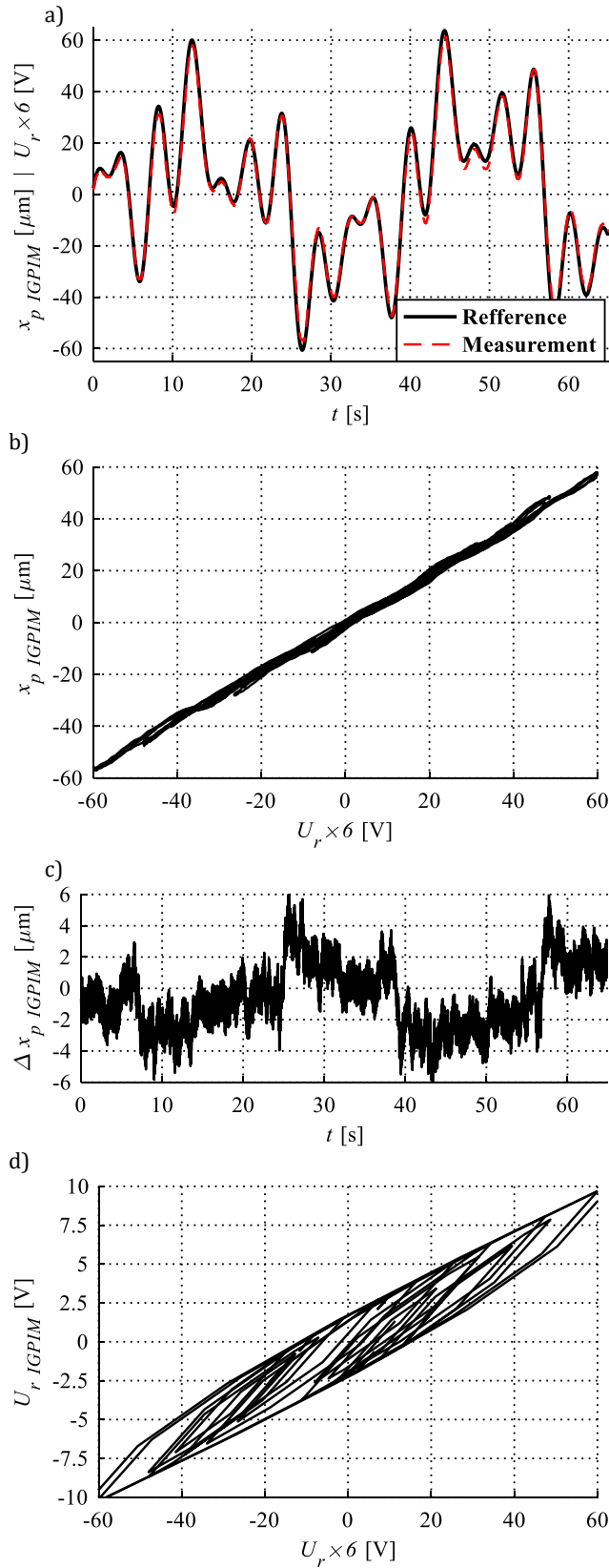


**Fig. 5.** Piezoelectric tube displacement for function F2 a) in time, b) for control voltage, c) modeling error in time, d) IGPIM model output.

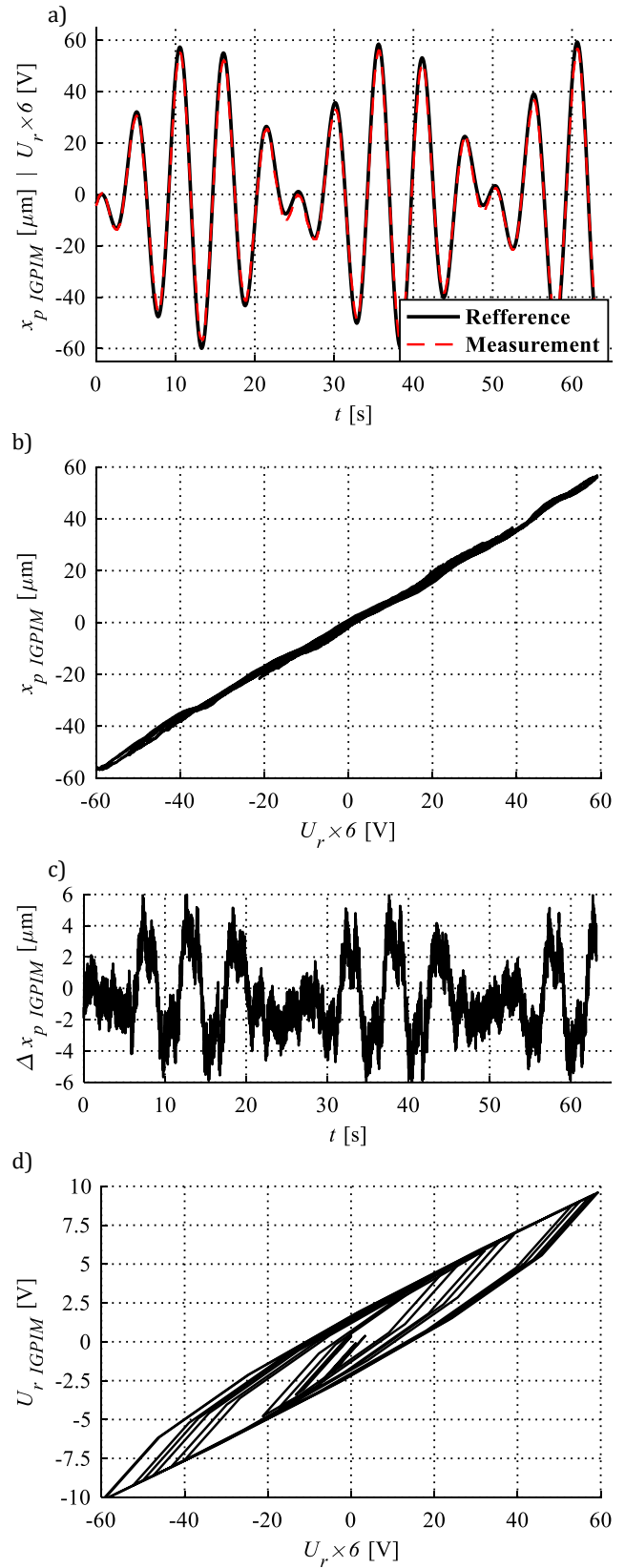


**Fig. 6.** Piezoelectric tube displacement for function F3 a) in time, b) for control voltage, c) modeling error in time, d) IGPIM model output.

Positioning accuracy of piezoelectric transducer in open loop control strategy with inverse hysteresis model strongly depends on the model accuracy. The modeling results presented in Fig. 2 and Table 1, show that in general, the error is very small and the maximal absolute value of the error equals 2.78  $\mu\text{m}$ , which is 2.34 % of the whole piezo tube movement range. Open loop control results for the same training signal as for model estimation was presented in Fig. 3. The max. absolute control error was 5.55  $\mu\text{m}$ , which is 4.56 % of the whole piezo tube range. Comparing results in Fig. 2 and Fig. 3 a significant reduction of the hysteresis can be seen. Since the model parameters were estimated on the training signal the control strategy should show best performance for this signal. For verification reason three other function were also tested. The control results for a much more complex verification input signal, very different from the training signal with various frequencies, still provide a small error. The maximal absolute error for signal F1 (Fig. 4) is 6.41  $\mu\text{m}$ , which is 5.55 % of the whole range. The maximal absolute error for signal F2 (Fig. 5) is 8.14  $\mu\text{m}$ , which is 6.75 % of the whole range. The maximal absolute error for signal F3 (Fig. 6) is 6.49  $\mu\text{m}$ , which is 5.6 % of the whole range.

Summarizing application of inverse hysteresis model in open loop control system of the piezoelectric actuator can reduce the hysteresis behavior and increase the positioning precision of the transducer.

#### ACKNOWLEDGEMENTS

The presented research results, executed under the subject of 02/22/DSPB/1208, were funded with grants for education allocated by the Ministry of Science and Higher Education in Poland.

#### REFERENCES

- [1] **Shan Y, Leang KK.** Accounting for hysteresis in repetitive control design: Nanopositioning example. *Automatica* 2012;48:1751-8.
- [2] **Gu G-Y, Zhu L-M, Su C-Y, Ding H, Fatikow S.** Modeling and Control of Piezo-Actuated Nanopositioning Stages: A Survey 2014;1-20.
- [3] **Moheimani SR, Fleming AJ.** Piezoelectric transducers for vibration control and damping. Springer Science & Business Media; 2006.
- [4] **Sędziak D.** Basic investigations of electrohydraulic servovalve with piezo-bender element. *Arch TechnolMaszAutom* 2006;26:185-90.
- [5] **Sangiah DK, Plummer AR, Bowen CR, Guerrier P.** A novel piezohydraulic aerospace servovalve. Part 1: Design and modelling. *Proc Inst MechEng Part J Syst Control Eng* 2013;227:371-89.
- [6] **Murrenhoff H.** Trends in valve development. *Inst Fluid Power Drives Controls IFAS* 2003.
- [7] **Ottman GK, Hofmann HF, Bhatt AC, Lesieutre GA.** Adaptive piezoelectric energy harvesting circuit for wireless remote power supply. *Power Electron IEEE Trans On* 2002;17:669-76.
- [8] **Priya S, Inman DJ.** Energy harvesting technologies. vol. 21. Springer; 2009.
- [9] **Janocha H.** Actuators. Springer; 2004.
- [10] **Janocha H.** Adaptronics and smart structures. Springer; 2007.
- [11] **Worden K, Haywood J.** Smart technologies. World Scientific; 2003.
- [12] **Hu H, Georgiou HMS, Ben-Mrad R.** Enhancement of tracking ability in piezoceramic actuators subject to dynamic excitation conditions. *IEEEASME Trans Mechatron* 2005;10:230-9.
- [13] **Su C-Y, Stepanenko Y, Svoboda J, Leung T-P.** Robust adaptive control of a class of nonlinear systems with unknown backlash-like hysteresis. *Autom Control IEEE Trans On* 2000;45:2427-32.
- [14] **Al Janaideh M, Rakheja S, Su C-Y.** Experimental characterization and modeling of rate-dependent hysteresis of a piezoceramic actuator. *Mechatronics* 2009;19:656-70.
- [15] **Al Janaideh M, Su C-Y, Rakheja S.** Development of the rate-dependent Prandtl-Ishlinskii model for smart actuators. *Smart Mater Struct* 2008;17:035026.
- [16] **Kuhnen K, Krejci P.** Compensation of complex hysteresis and creep effects in piezoelectrically actuated systems - a new Preisach modeling approach. *Autom Control IEEE Trans On* 2009;54:537-50.
- [17] **Al Janaideh M, et al.** Generalized Prandtl-Ishlinskii hysteresis model: Hysteresis modeling and its inverse for compensation in smart actuators. *W Decision and Control, 2008. CDC 2008. 47th IEEE Conference on. IEEE, 2008. p. 5182-5187.*
- [18] **Al Janaideh M, et al.** Invers egeneralized asymmetric Prandtl-Ishlinskii model for compensation of hysteresis nonlinearities in smart actuators. *W Networking, Sensing and Control, 2009. ICNSC'09. International Conference on. IEEE, 2009. p. 834-839.*
- [19] **Al Janaideh M, SU A, Chun-Yi, Rakheja S.** Compensation of symmetric and asymmetric hysteresis nonlinearities in smart actuators with a generalized Prandtl-Ishlinskii presentation. *W Advanced Intelligent Mechatronics (AIM), 2010 IEEE/ASME International Conference on. IEEE, 2010. p. 890-895.*